Formation of Isolated Zn Vacancies in ZnO Single Crystals by Absorption of Ultraviolet Radiation: A Combined Study Using Positron Annihilation, Photoluminescence, and Mass Spectroscopy

Enamul H. Khan,[1,*] Marc H. Weber,[2] and Matthew D. McCluskey[1]

[1]*Department of Physics and Astronomy, Washington State University, Pullman, Washington 99164-2814, USA*
[2]*Center for Materials Research, Washington State University, Pullman, Washington 99164-2711, USA*

(Received 4 February 2013; published 2 July 2013)

Positron annihilation spectra reveal isolated zinc vacancy (V_{Zn}) creation in single-crystal ZnO exposed to 193-nm radiation at 100 mJ/cm^2 fluence. The appearance of a photoluminescence excitation peak at 3.18 eV in irradiated ZnO is attributed to an electronic transition from the V_{Zn} acceptor level at ~100 meV to the conduction band. The observed V_{Zn} density profile and hyperthermal Zn^+ ion emission support zinc vacancy-interstitial Frenkel pair creation by exciting a wide 6.34 eV Zn-O antibonding state at 193-nm photon—a novel photoelectronic process for controlled V_{Zn} creation in ZnO.

DOI: 10.1103/PhysRevLett.111.017401 PACS numbers: 78.40.Fy, 71.55.Gs, 78.70.Bj, 79.20.Ds

ZnO is an important transparent semiconducting material that has generated significant research interest [1–3]. A recent review of defects in ZnO by McCluskey and Jokela [2] has highlighted the need to understand the role of various defects on the electronic properties of ZnO. First-principles calculations place the $0/-1$ acceptor level of the zinc vacancy (V_{Zn}) 100 meV above the valence band maximum [4,5]. Therefore, V_{Zn} creation by equilibrium or nonequilibrium processes may become an initial step toward obtaining *p*-type ZnO. Since positrons are sensitive to neutral or negatively charged open volume V_{Zn} defects, positron annihilation spectroscopy (PAS) has been used extensively to study V_{Zn} in ZnO. Early PAS work on energetic particle irradiated ZnO demonstrated V_{Zn} formation in isolated or complex states depending on irradiation parameters like dose, energy, and type of incident particle [6–10].

Energetic particle irradiation generally produces vacancies and interstitials on both sublattices [11], and often forms undesired complexes, thus limiting its ability to create isolated V_{Zn} [10]. In principle, annealing in oxygen could generate V_{Zn} defects, but this process is controlled by thermodynamics and may not produce a sufficiently high concentration. Mechanical treatments, such as polishing or indenting, have also created subsurface defects like V_{Zn} in single crystal ZnO [12–14]. Defect creation in such nonthermal mechanical treatments is uncontrollable. On the other hand, optical excitation is an efficient and controlled nonthermal defect creation process for many materials. For example, optical excitations produce color centers in alkali halides due to their large self-trapping potentials for excitons [15].

In oxide systems, there is a potential barrier between the exciton self-trapping and defect pair creation [15]. The well-documented radiation hardness of ZnO also suggests that it is resilient to defect formation. However, a recent study of Zn^+ ion emission predicts V_{Zn} creation upon irradiation with 193 nm excimer laser light [16]. If the predicted V_{Zn} creation does occur, then it must be due to a novel photoelectronic process. This process could open up the possibility of controlled incorporation of point defects. Therefore, studies of 193 nm photonic interactions with single crystal ZnO encompass fundamental as well as applied research.

This Letter presents evidence for isolated V_{Zn} creation following 193 nm excimer laser interactions with single-crystal ZnO. PAS shows isolated V_{Zn} defects creation in the irradiated material. Diffusion of zinc interstitials to the surface could leave behind isolated V_{Zn} defects and promote surface sensitive Zn^+ ion desorption, presumably due to zinc interstitial-vacancy Frenkel pair creation by selective excitation of Zn-O bond. Appearance of a photoluminescence excitation (PLE) peak at 3.18 eV in irradiated material suggests that the isolated V_{Zn} defects have a shallow 100 meV acceptor state.

The ZnO single crystals, grown by a chemical vapor transport method, were nominally *n* type with a free-electron sheet concentration of ~10^{13} cm^{-2}. As-grown platelet type samples, 0.2–1 mm thick, were used in this study. The sample excitation was performed under ultra-high vacuum (UHV) conditions (~1×10^{-8} Pa) at 100 or 400 mJ/cm^2 fluence of 193 nm excimer laser pulses, each 20 ns wide, at a 1 Hz repetition rate. Zn^+ ion time-of-flight (TOF) signals were acquired with a UTI-100C quadrupole mass spectrometer (QMS) that passes only Zn^+ ions when tuned to mass resonance of 64 amu/*e* [17]. A 32-cm long free flight distance was set for the Zn^+ ion TOF.

Positron measurements were carried out with the WSU monoenergetic variable energy positron beam. Depth resolved PAS results were extracted from the Doppler broadening of the 511 keV annihilation line with an energy resolution of 1.4 keV (full width half maximum) and are expressed in terms of the *S* and *W* parameters [18]. The *S* parameter comprises the central fraction of the positron annihilation peak at 511 keV where lower momentum

Doppler shifts dominate. It is sensitive to neutral or negatively charged vacancies with reduced concentration of high momentum electrons. The W parameter comprises the wings of the peak where higher momentum Doppler shifts dominate. It relates to the chemical environment of an annihilation site. The S and W parameters were normalized to the as-grown pristine state values of 0.4039 ± 0.0002 and 0.1059 ± 0.0001, respectively, at a depth in excess of 2 μm.

PLE spectroscopy was performed using a JY-Horiba FluoroLog-3 spectrofluorometer equipped with double grating monochromators (1200 grooves/mm), and a R928P photomultiplier tube. A xenon 450 W lamp was used for excitation. Free carrier absorption was obtained with a Bomem DA8 vacuum Fourier transform infrared (FTIR) spectrometer equipped with a Globar light source, a KBr beam splitter, and a liquid-nitrogen-cooled HgCdTe detector. A Janis closed-cycle helium cryostat system maintained the sample temperature.

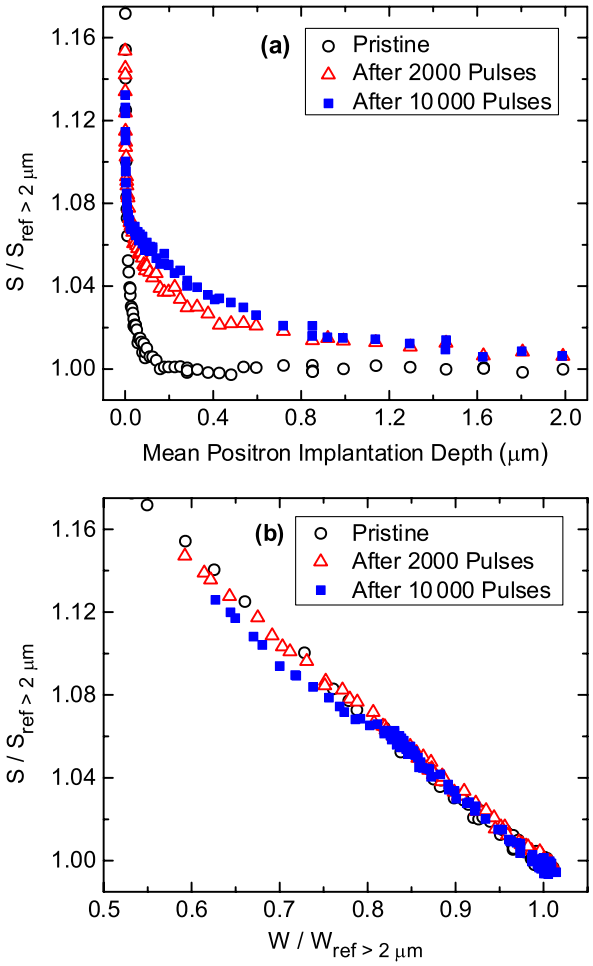

FIG. 1 (color online). (a) PAS S parameter versus mean implantation depth and (b) corresponding S-W parameter plots for single crystal ZnO before 193 nm laser irradiation, after 2000 pulses, and after 10 000 pulses. The irradiation was performed at 100 mJ/cm^2 fluence per pulse under UHV conditions.

Figure 1(a) shows the S parameter versus mean positron implantation depth for an as-grown sample as a function of radiation exposure performed at 100 mJ/cm^2 fluence. The S parameter value at the surface, in general, reflects positronium formation with surface electrons [18]. At greater depths, the S parameter value in ZnO primarily reflects zinc vacancies [6], even though it could also reflect the concentration of divacancies or complexes [14,19]. In unirradiated pristine ZnO, the S values near the surface, represented by open circles, drop quickly to a plateau at increasing depths. This sharp drop to the bulk S value of 0.4039 ± 0.0002 reflects a reference baseline for low concentration of V_{Zn} point defects in pristine ZnO.

The sample was then irradiated to 2000 pulses. In this initial irradiated state, the S parameter remains significantly above the baseline, indicating open volume defect creation in the near surface region [Fig. 1(a)]. In addition, the corresponding S-W parameter curves in Fig. 1(b) show the same straight line trend for the pristine and initial irradiated states, indicating that irradiation creates the same kind of defects originally present in the pristine state. The observed (S, W) values in the initial irradiated state are consistent with the published (S, W) values for isolated V_{Zn}. The published (S, W) values represent a range (1.04–1.05, 0.87–0.79) depending on experimental configuration [6,7,9]. The increased S values below the surface in the initial irradiated state, and the slope of the S-W lines in the pristine and initial irradiated states, are consistent with formation of isolated V_{Zn} defects [6]. Therefore, the PAS results suggest that 193 nm excitation produces isolated V_{Zn} defects in single-crystal ZnO. Moreover, the S parameter in the initial irradiated state extends more than 2 μm into the bulk material, indicating the presence of isolated V_{Zn} defects in the bulk.

The sample was further irradiated to a total of 10 000 pulses. In this final irradiated state, the S parameter is only slightly higher than in the initial irradiated state [Fig. 1(a)]. While further increment of S values in final irradiated state might suggest more isolated V_{Zn} creation, the corresponding S-W curve in Fig. 1(b) does not follow the straight line trend previously obtained on the pristine and initial irradiated states, likely due to saturation. Saturation positron trapping can occur for two reasons. First, if the isolated V_{Zn} concentration reaches a critical level (high 10^{18} cm^{-3}), and all positrons annihilate at these defects. Second, if open volume defects with larger trapping coefficients are created, positrons may annihilate at these defects instead of V_{Zn} defects.

To understand the nature of the observed saturation, VEPFIT analysis that incorporated three layers (top 100–150 nm, mid 200–700 nm, and the bulk) was performed. The results are shown in Fig. 2. The VEPFIT results for initial and final irradiated states, represented by stars, clearly pass through the black line, which connects Tuomisto's experimental result for the isolated V_{Zn} defects,

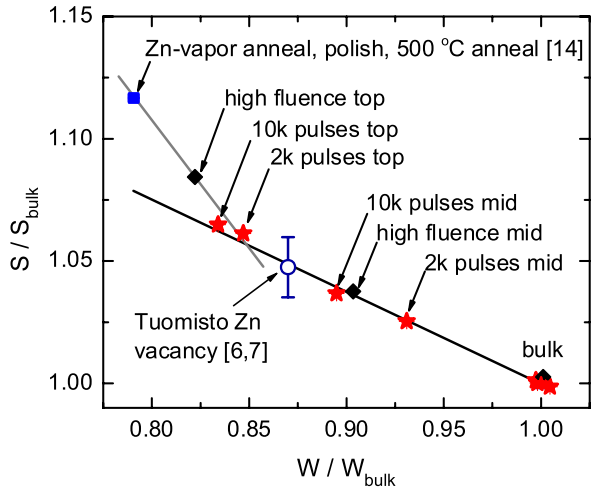

FIG. 2 (color online). PAS results calculated using the VEPFIT model, incorporating two thin layers (top, mid) and bulk. The open circle shows Tuomisto's experimental result for the isolated Zn vacancy [6,7]. Stars show isolated Zn vacancies created by laser exposure at 100 mJ/cm^2 fluence excitation. Diamonds show large open volume defects creation in the top layer (100–150 nm) at high fluence (400 mJ/cm^2) excitation.

open circle, and the referenced bulk defects. This black line represents an increasing concentration of isolated V_{Zn} defects with respect to the bulk. This analysis indicates only isolated V_{Zn} creation during 193 nm photonic excitation, and demonstrates a controlled V_{Zn} fabrication near the saturation concentrations for positrons. Assuming a bulk positron lifetime of 170 ps [6], a trapping coefficient of $3\times10^{15}\,s^{-1}$, and an atomic density of 8.3×10^{22} cm^{-3}, an estimate for the V_{Zn} concentration can be made. The 2000-pulse initial irradiation creates 1.4×10^{18} and 5.5×10^{16} cm^{-3} zinc vacancies in the top and middle layers, respectively; the 10 000-pulse total irradiation increases these concentrations to 2.2×10^{19} and 1.2×10^{17} cm^{-3}, respectively.

The same analysis was performed on another sample irradiated to 2000 pulses at high fluence (400 mJ/cm^2). The corresponding VEPFIT results are shown by diamonds in Fig. 2. A clear deviation from the black line is noticed for the top layer, heading toward Selim's experimental result for larger defects in ZnO [14]. The large open volume defect creation can be understood from the perspective of significant neutral particle (atomic Zn and O) emission during the laser pulse. At high fluence, a detected particle emission rate of ~0.1 monolayer per pulse is consistent with leaving behind large open volume defects [20]. On the other hand, during low fluence excitation, the neutral particle emission rate falls below 10^{-9} monolayer per pulse [20]. The lack of detectable neutral particle emission for ZnO under low fluence excitation correlates with only isolated V_{Zn} creation.

The low fluence PAS results reveal the highest concentration of isolated V_{Zn} defects in the top layer, which overlaps with absorption depth for 193 nm photons in ZnO ($d_{Ab}\sim200$ nm). The dominant V_{Zn} presence in the top layer is consistent with 193 nm photons creating these defects in the interaction layer, defined by laser absorption depth. The increased V_{Zn} presence in the middle layer and beyond is likely related to a secondary response induced by the laser pulse. Transient laser heating can trigger diffusion of newly created V_{Zn} in the interaction volume. A diffusion penetration depth can be estimated by $d_{th}=\sqrt{\alpha\tau}$, where $\alpha=0.8$ cm^2/s is the thermal diffusivity of single crystal ZnO [21], and $\tau=20$ ns is the laser pulse duration. An approximate value of $d_{th}\sim1$ μm allows the transient thermal field to extend about a few μm into the bulk, which is consistent with the observed V_{Zn} density profile, indicating that diffusion of the newly created defects is likely occurring.

The transient temperature rise can be estimated by $\Delta T=2(1-R)(F/k)(\alpha/\pi\tau)^{1/2}$ [22]. Here $k\approx1$ W cm^{-1} K^{-1} is the thermal conductivity of single-crystal ZnO [23], and $R\approx0.12$ is the reflectivity of ZnO at 193 nm [24]. At $F=100$ mJ/cm^2 fluence, the transient temperature rises to ~200 °C. After characterizing the final irradiation state, the sample was also annealed at 200 °C for one hour under UHV conditions. Subsequent PAS measurement showed a slightly more pronounced drop in the V_{Zn} density profile, indicating that the V_{Zn} defects are almost distributed by transient heating, and, therefore, are relatively immobile up to 200 °C anneal. Considering extremely fast diffusion time scale (d_{Ab}^2/α), about a few ns, a ~200 °C transient heating seems sufficient to diffuse point defects created in ZnO [25,26].

Surface defects can act as a sink for the diffusing interstitial zinc ions (Zn_i^+) created during laser pulse by 193 nm photonic excitation. Upon reaching the surface, a Zn_i^+ ion could find a neutral surface oxygen vacancy site and adsorb as a weakly bound surface defect complex, which acts as an ideal source for ion emission during excimer laser interaction [16,17,27]. Ion desorption experiments performed on a ZnO sample during 100 mJ/cm^2 fluence excitation under UHV conditions result in only Zn^+ ion emission shown by the TOF (Fig. 3). A Gaussian fit to the TOF [16] yields a mean kinetic energy of ~6 eV for the emitted Zn^+ ion distribution. A simple electrostatic model can explain this hyperthermal emission mechanism that requires photoionization of the oxygen vacancy of such a surface defect complex [16,17,27]. This photoionization step immediately switches the weakly bound complex into a repulsive center. The repulsive Coulomb force between the Zn^+ ion and positively charged oxygen vacancy emits the Zn^+ ion with hyperthermal energies. In ZnO, a 0.21 nm oxygen vacancy to adsorbed Zn^+ ion effective bond length can deliver up to 6.9 eV of maximum kinetic energy [16], which is consistent with the observed mean kinetic energy of 6 eV.

The formation of such surface defect complexes, due to Zn_i^+ transport to the surface, could affect the ion yield.

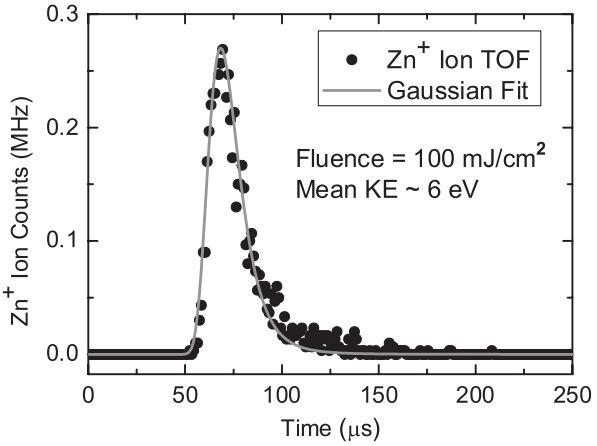

FIG. 3. The 193 nm interaction leads into only hyperthermal Zn^+ ion emission from ZnO surface under UHV conditions at 100 mJ/cm^2 fluence. The Zn^+ ion TOF was acquired at 64 amu/e mass resonance and best QMS mass resolution.

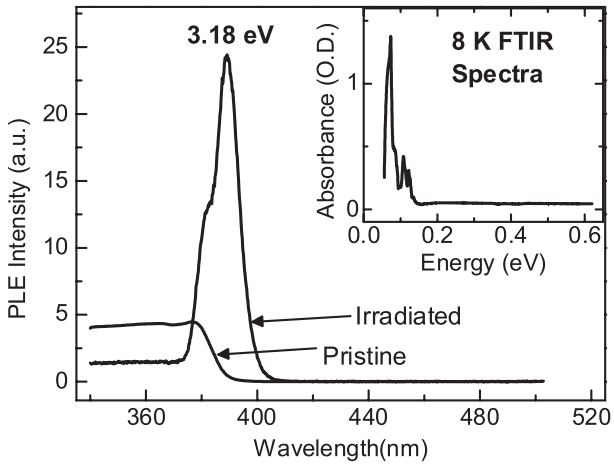

FIG. 4. 193 nm irradiation effect on room temperature PLE spectra for 525 nm emission. The 525 nm emission was collected at 1 nm resolution while the sample was excited in steps of 0.2 nm at 0.5 nm resolution. Inset shows an 8 K FTIR spectrum of the irradiated sample. Irradiation was performed at 100 mJ/cm^2 fluence for 2000 pulses under UHV conditions.

A Zn^+ ion emission study on ZnO at 193 nm interaction has demonstrated nearly exponential decay of Zn^+ ion yield as a function of exposure at fluences ≤ 40 mJ/cm^2 [16]. The first order exponential decay kinetics reflect only consumption of such preexisting surface defect complexes via emission process. On the other hand, the decay kinetics change to a second order at fluences ≥ 60 mJ/cm^2 [16], reflecting replenishment of such defect complexes due to Zn_i^+ ion transport to the surface. The observed V_{Zn} density profile and Zn^+ ion emission with second order decay kinetics verify the diffusion driven distribution of these defects. Besides, this study and the previous one observe only Zn^+ ion emission at fluences ≤ 100 mJ/cm^2, and could not verify oxygen ion emission despite a near unity ion detection sensitivity [16]. Therefore, preferential Zn^+ ion emission and V_{Zn} creation suggest that selective photoelectronic $Zn_i - V_{Zn}$ Frenkel pair creation occurs during 193 nm irradiation.

Transient heating at 200 °C is not sufficient to create such a Frenkel pair in ZnO. In alkali halides, Frenkel pairs are produced via large exciton self-trapping potentials [15]. ZnO, in contrast, does not exhibit exciton self-trapping. Interestingly, ZnO single crystal shows a wide 6.34 eV transition associated with hybridized O $2p$ and Zn $4sp$ atomic orbitals [28–31]. If the electron wave function has nodes between the Zn and O atoms, it would be strongly antibonding. Thus, the absorption of one 6.4 eV photon could excite this wide antibonding state of the Zn-O bond parallel to the crystal c axis. This excitation could then break the bond and create a Frenkel pair in the Zn sublattice.

The zinc vacancy is an acceptor with a theoretical predicted $0/-1$ transition state at 100 meV above the valence band maximum [4,5]. In order to investigate the electronic state of the isolated V_{Zn} defects, the PLE technique was employed, since PL in ZnO is a surface sensitive probe under ultraviolet excitation. Pristine and irradiated samples showed a green PL band peaked at 525 nm under steady-state ultraviolet excitation. PLE spectra for 525 nm emission are shown in Fig. 4. In the pristine state, the PLE spectrum behaves like a step function, essentially following the fundamental absorption edge. The flat response over the 340–378 nm range suggests that electron-hole pair excitation at energies higher than 3.28 eV (378 nm) efficiently produce green emission. Above 378 nm excitation, the green emission intensity falls sharply to zero, demonstrating that excitation energies less than 3.28 eV do not produce green emission in the pristine state.

For the irradiated sample, the PLE spectrum at energies less than 3.28 eV is dramatically different. An excitation band appears at ~3.18 eV (389.5 nm), confirming a new defect band that acts as source for 525 nm green emission. This 3.18 eV defect absorption band is ~100 meV below the room-temperature band gap of ZnO. This 3.18 eV absorption band is tentatively assigned to an electron transfer from the V_{Zn} $0/-1$ acceptor level to the conduction band minimum. The appearance of a V_{Zn} related band in irradiated material is consistent with creation of mostly localized defects, which is verified by the absence of any free carrier absorption in the 8 K FTIR absorption spectrum shown in the inset. The fact that 193 nm excitation does not produce significant free carrier densities at 8 K suggests that it might be possible to produce V_{Zn} defects that are not accompanied by compensating donor defects.

In conclusion, evidence is presented for the controlled formation of isolated zinc vacancies during 193 nm excimer laser irradiation at 100 mJ/cm^2 fluence. The stable zinc vacancies are associated with a shallow acceptor level about 100 meV above the valence band maximum. The ability to produce relatively high densities of zinc

vacancies in the subsurface material may prove useful in tailoring the electronic properties of zinc oxide—either directly, by providing acceptor defects, or indirectly, by stabilizing implanted dopants.

This work was supported by the U.S. Department of Energy under Contracts No. DE-FG02-04ER-15618 and No. DE-FG02-07ER-46386 (M. D. M.). M. H. Weber and the positron work were supported by the Army Research Laboratory under Contract No. W9113M-09-0075. We thank Dr. L. A. Boatner for providing the crystals grown at the Oak Ridge National Laboratory. E. H. Khan specially thanks his Ph.D. advisor, Prof. J. T. Dickinson, for allowing him to work on this collaborative project independently. M. C. Tarun helped with the initial PLE experimental work.

*Corresponding author.
enamul_khan@wsu.edu

[1] Ü. Özgür, Ya. I. Alivov, C. Liu, A. Teke, M. A. Reshchikov, S. Doğan, V. Avrutin, S.-J. Cho, and H. Morkoç, J. Appl. Phys. **98**, 041301 (2005).
[2] M. D. McCluskey and S. J. Jokela, J. Appl. Phys. **106**, 071101 (2009).
[3] A. Janotti and C. G. Van de Walle, Rep. Prog. Phys. **72**, 126501 (2009).
[4] A. F. Kohan, G. Ceder, D. Morgan, and C. G. Van deWalle, Phys. Rev. B **61**, 15019 (2000).
[5] A. Janotti and C. G. Van de Walle, Phys. Rev. B **76**, 165202 (2007).
[6] F. Tuomisto, V. Ranki, K. Saarinen, and D. C. Look, Phys. Rev. Lett. **91**, 205502 (2003).
[7] F. Tuomisto, K. Saarinen, D. C. Look, and G. C. Farlow, Phys. Rev. B **72**, 085206 (2005).
[8] Z. Q. Chen, S. J. Wang, M. Maekawa, A. Kawasuso, H. Naramoto, X. L. Yuan, and T. Sekiguchi, Phys. Rev. B **75**, 245206 (2007).
[9] A. Zubiaga, F. Tuomisto, V. A. Coleman, H. H. Tan, C. Jagadish, K. Koike, S. Sasa, M. Inoue, and M. Yano, Phys. Rev. B **78**, 035125 (2008).
[10] Y. F. Dong, F. Tuomisto, B. G. Svensson, A. Y. Kuznetsov, and L. J. Brillson, Phys. Rev. B **81**, 081201 (2010).
[11] F. Tuomisto, V. Ranki, D. C. Look, and G. C. Farlow, Phys. Rev. B **76**, 165207 (2007).
[12] Z. Takkouk, N. Brihi, K. Guergouri, and Y. Marfaing, Physica (Amsterdam) **366B**, 185 (2005).
[13] Y. Ohno, H. Koizumi, T. Taishi, I. Yonenaga, K. Fujii, H. Goto, and T. Yao, Appl. Phys. Lett. **92**, 011922 (2008).
[14] F. A. Selim, M. H. Weber, D. Solodovnikov, and K. G. Lynn, Phys. Rev. Lett. **99**, 085502 (2007).
[15] N. Itoh and A. M. Stoneham, *Materials Modification by Electronic Excitation* (Cambridge University Press, Cambridge, England, 2001), pp. 4 and 224.
[16] E. H. Khan, S. C. Langford, J. T. Dickinson, and L. A. Boatner, J. Appl. Phys. **111**, 063101 (2012).
[17] J. T. Dickinson, S. C. Langford, J. J. Shin, and D. L. Doering, Phys. Rev. Lett. **73**, 2630 (1994).
[18] P. J. Schultz and K. G. Lynn, Rev. Mod. Phys. **60**, 701 (1988).
[19] M. H. Weber, F. A. Selim, D. Solodovnikov, and K. G. Lynn, Appl. Surf. Sci. **255**, 68 (2008).
[20] E. H. Khan *et al.*, J. Appl. Phys. (to be published).
[21] X.-D. Xu, D. Ma, S.-Y. Zhang, A.-H. Luo, and W. Kiyotaka, Chin. Phys. Lett. **25**, 176 (2008).
[22] E. H. Khan, S. C. Langford, J. T. Dickinson, L. A. Boatner, and W. P. Hess, Langmuir **25**, 1930 (2009).
[23] Ü. Özgür, X. Gu, S. Chevtchenko, J. Spradlin, S.-J. Cho, H. Morkoç, F. H. Pollak, H. O. Everitt, B. Nemeth, and J. E. Nause, J. Electron. Mater. **35**, 550 (2006).
[24] J. L. Freeouf, Phys. Rev. B **7**, 3810 (1973).
[25] L. S. Vlasenko and G. D. Watkins, Phys. Rev. B **71**, 125210 (2005).
[26] P. Erhart and K. Albe, Appl. Phys. Lett. **88**, 201918 (2006).
[27] E. Khan, S. Langford, and J. Dickinson, J. Appl. Phys. **110**, 023110 (2011).
[28] A. Kobayashi, O. F. Sankey, S. M. Volz, and J. D. Dow, Phys. Rev. B **28**, 935 (1983).
[29] P. J. Moller, S. Komolov, and E. Lazneva, J. Phys. Condens. Matter **11**, 9581 (1999).
[30] P. S. Xu, Y. M. Sun, C. S. Shi, F. Q. Xu, and H. B. Pan, Nucl. Instrum. Methods Phys. Res., Sect. B **199**, 286 (2003).
[31] K. Ozawa, K. Sawada, Y. Shirotori, K. Edamoto, and M. Nakatake, Phys. Rev. B **68**, 125417 (2003).